

Interpreting NO ν A and T2K data in the presence of a light sterile neutrino

Sabya Sachi Chatterjee¹ and Antonio Palazzo^{2,3}

¹ *Institute for Particle Physics Phenomenology, Department of Physics, Durham University, Durham, DH1 3LE, UK*

² *Dipartimento Interateneo di Fisica “Michelangelo Merlin,” Via Amendola 173, 70126 Bari, Italy*

³ *Istituto Nazionale di Fisica Nucleare, Sezione di Bari, Via Orabona 4, 70126 Bari, Italy*

We study in detail the impact of a light sterile neutrino in the interpretation of the latest data of the long baseline experiments NO ν A and T2K, assessing the robustness/fragility of the estimates of the standard 3-flavor parameters with respect to the perturbations induced in the 3+1 scheme. We find that the 3-flavor ($\sim 2.4\sigma$) indication in favor of the normal ordering remains almost unaltered in the 4-flavor scheme ($\sim 2.2\sigma$). We also show that, in the (preferred) normal neutrino ordering, the indication in favor of CP-violation found in the 3-flavor framework ($\sim 2.0\sigma$) appreciably decreases in the 3+1 scheme ($\sim 1.2\sigma$). Regarding the atmospheric mixing angle θ_{23} , the preference for the higher octant of θ_{23} shows a sensible reduction in the presence of a sterile neutrino ($\sim 1.7\sigma$ vs $\sim 1.0\sigma$). Our analysis also demonstrates that it is possible to attain constraints on the new CP-phase δ_{14} , which interestingly has best fit value close to that of the standard CP phase δ_{13} . Finally, we highlight a striking positive correlation among the standard CP-phase δ_{13} and the new CP-phase δ_{14} .

I. INTRODUCTION

Neutrino mass and mixing have been firmly established by several experiments using natural and artificial neutrino sources. The 3-flavor framework is recognized as the sole scheme able to describe all the measurements obtained at baselines longer than ~ 100 meters. Despite its huge success, however, the standard 3-flavor scheme does not need to constitute the ultimate description of neutrino properties. As a matter of fact, several anomalies have been found in short baseline experiments (SBL), which cannot be described in the 3-flavor scenario (for reviews on the subject see [1–10]). The hints derive from the accelerator experiments LSND [11] and MiniBooNE [12], and from the so-called reactor [13] and Gallium [14, 15] anomalies. More recently, the nuclear reactor data from NEOS [16], DANSS [17] and Neutrino-4 [18], have provided indications in the same direction. Limits on light sterile neutrinos have been also found exploiting solar neutrinos [19–21], the long-baseline (LBL) experiments MINOS, MINOS+ [22, 23], NO ν A [24] and T2K [25], the reactor experiments Daya Bay [26], PROSPECT [27] and STEREO [28], and also the atmospheric data collected at Super-Kamiokande [29], IceCube [30, 31] and ANTARES [32].

In the 3-flavor framework three mass eigenstates ν_i with masses m_i ($i = 1, 2, 3$) are introduced, together with three mixing angles ($\theta_{12}, \theta_{23}, \theta_{13}$), and one CP-phase δ_{13} . The neutrino mass ordering (NMO) is dubbed normal (NO) if $m_3 > m_{1,2}$ or inverted (IO) if $m_3 < m_{1,2}$. The two mass-squared splittings $\Delta m_{21}^2 \equiv m_2^2 - m_1^2$ and $\Delta m_{31}^2 \equiv m_3^2 - m_1^2$ are too small to give rise to detectable effects in SBL setups. Therefore, new neutrino species, having much bigger mass-squared differences $O(\text{eV}^2)$ must be introduced to explain the SBL anomalies. The new hypothetical neutrino states are assumed to be sterile, i.e. singlets of the standard model gauge group. Several new and more sensitive SBL experiments are underway to put under test such an intriguing hypothesis (see the review in [6]), which, if confirmed would constitute a tangible evidence of physics beyond the standard model. In the minimal extension of the 3-flavor framework, the so-called 3 + 1 scheme, only one sterile species is introduced. In this scenario, one supposes that one mass eigenstate ν_4 exists, weakly mixed with the active neutrino flavors (ν_e, ν_μ, ν_τ) and separated from the standard mass eigenstates (ν_1, ν_2, ν_3) by a $O(\text{eV}^2)$ difference. The 3+1 framework is governed by six mixing angles and three (Dirac) CP-violating phases. Therefore, in the eventuality of a discovery of a light sterile species, we would face the challenging task of identifying six new properties [3 mixing angles ($\theta_{14}, \theta_{24}, \theta_{34}$), 2 CP-phases (δ_{14}, δ_{34}), and the mass-squared splitting $\Delta m_{41}^2 \equiv m_4^2 - m_1^2$].

As first pointed out in Ref. [33], in the presence of a light sterile neutrino, the $\nu_\mu \rightarrow \nu_e$ conversion probability probed by the long baseline (LBL) facilities entails a new term engendered by the interference among the atmospheric frequency and the new frequency connected to the sterile species. The oscillations induced by the new frequency are very fast and are completely smeared out by the finite energy resolution of the detector. Notwithstanding, the fourth neutrino leaves observable traces in the conversion probability. This makes the LBL experiments able to probe the new CP-phases entailed by the 3+1 scheme. The recent 4-flavor analyses of NO ν A and T2K data, have already pointed out that such two experiments have some sensitivity to one of such CP-phases [7, 33, 34]. Likewise, the sensitivity study carried out in [35] has pointed out that the discovery potential of the CP-phases is expected to increase when NO ν A and T2K will attain their final exposures, and will be further improved in the new-generation LBL facilities DUNE [36–42], T2HK [42–44], T2HKK [42, 45], and ESS ν SB [46] (for a recent review on the topic see Ref. [47]). In this work, we analyze the latest data provided by NO ν A and T2K, and we assess the robustness of the 3-flavor estimates of the oscillation parameters in the enlarged 3+1 scheme. In addition, we analyze the indications on the new

CP-phase δ_{14} . Further studies on the the impact of sterile neutrinos in LBL experiments, mostly focused on future experiments, can be found in [48–56]. We underline that while this work deals with charged current interactions, one can obtain valuable information on active-sterile oscillations parameters also from the analysis of neutral current interactions (see [22–25] for constraints from existing data and [41, 57] for sensitivity studies of future experiments).

II. THEORETICAL FRAMEWORK

In the presence of a sterile neutrino, the flavor $(\nu_e, \nu_\mu, \nu_\tau, \nu_s)$ and the mass eigenstates $(\nu_1, \nu_2, \nu_3, \nu_4)$ are mixed by a 4×4 unitary matrix

$$U = \tilde{R}_{34} R_{24} \tilde{R}_{14} R_{23} \tilde{R}_{13} R_{12}, \quad (1)$$

with R_{ij} (\tilde{R}_{ij}) representing a real (complex) 4×4 rotation of a mixing angle θ_{ij} which endows the 2×2 submatrix

$$R_{ij}^{2 \times 2} = \begin{pmatrix} c_{ij} & s_{ij} \\ -s_{ij} & c_{ij} \end{pmatrix}, \quad \tilde{R}_{ij}^{2 \times 2} = \begin{pmatrix} c_{ij} & \tilde{s}_{ij} \\ -\tilde{s}_{ij}^* & c_{ij} \end{pmatrix}, \quad (2)$$

in the (i, j) sub-block. For compactness, we have defined

$$c_{ij} \equiv \cos \theta_{ij}, \quad s_{ij} \equiv \sin \theta_{ij}, \quad \tilde{s}_{ij} \equiv s_{ij} e^{-i\delta_{ij}}. \quad (3)$$

The matrix in Eq. (1) possesses some useful properties: i) The 3-flavor matrix is recovered if one sets $\theta_{14} = \theta_{24} = \theta_{34} = 0$. ii) For small values of the mixing angles θ_{14} , θ_{24} , and θ_{13} , it is $|U_{e3}|^2 \simeq s_{13}^2$, $|U_{e4}|^2 = s_{14}^2$, $|U_{\mu 4}|^2 \simeq s_{24}^2$, and $|U_{\tau 4}|^2 \simeq s_{34}^2$, with a clear physical interpretation of the three mixing angles. iii) The leftmost positioning of the matrix \tilde{R}_{34} guarantees that the $\nu_\mu \rightarrow \nu_e$ probability in vacuum is independent of θ_{34} and of the associated CP phase δ_{34} (see [33]).

For simplicity, we limit our treatment to the case of oscillations in vacuum.¹ As first shown in [33], the $\nu_\mu \rightarrow \nu_e$ probability can be expressed as the sum of three terms

$$P_{\mu e}^{4\nu} \simeq P^{\text{ATM}} + P_1^{\text{INT}} + P_{\text{II}}^{\text{INT}}. \quad (4)$$

The first term, which is positive-definite, is related solely to the atmospheric mass-squared splitting and gives the biggest contribution to the probability. It can be cast in the form

$$P^{\text{ATM}} \simeq 4s_{23}^2 s_{13}^2 \sin^2 \Delta, \quad (5)$$

where $\Delta \equiv \Delta m_{31}^2 L / 4E$ is the atmospheric oscillating factor, L and E being the neutrino baseline and energy, respectively. The other two terms in Eq. (4) are generated by the interference of two frequencies and are not positive-definite. In particular, the second term in Eq. (4) arises from the interference of the solar and atmospheric frequencies and can be expressed as

$$P_1^{\text{INT}} \simeq 8s_{13}s_{12}c_{12}s_{23}c_{23}(\alpha\Delta)\sin\Delta\cos(\Delta+\delta_{13}), \quad (6)$$

where we have defined the ratio of the solar over the atmospheric mass-squared splitting, $\alpha \equiv \Delta m_{21}^2 / \Delta m_{31}^2$. We recall that at the first oscillation maximum it is $\Delta \sim \pi/2$. The third term in Eq. (4) appears as a new genuine 4-flavor effect, and it arises from the interference of the atmospheric frequency with the new frequency introduced by fourth mass eigenstate. This term can be cast in the form [33]

$$P_{\text{II}}^{\text{INT}} \simeq 4s_{14}s_{24}s_{13}s_{23}\sin\Delta\sin(\Delta+\delta_{13}-\delta_{14}). \quad (7)$$

From inspection Eqs. (5)-(7), one can notice that the probability depends (besides the large mixing angle θ_{23}) on three small mixing angles: θ_{13} , θ_{14} and θ_{24} . One can notice that the values of such three mixing angles (estimated in the 3-flavor scenario [58–60] for θ_{13} , and in the 4-flavor framework [7–10] for θ_{14} and θ_{24}) are similar as one has $s_{13} \sim s_{14} \sim s_{24} \sim 0.15$. Therefore, one is legitimate to consider these three angles as small quantities of the same order of magnitude ϵ . We also note that $|\alpha| \simeq 0.03$, can be considered of order ϵ^2 . Hence, Eqs. (5)-(7), show that the first (leading) contribution is of the second order, while each of the two interference terms is of the third order.

¹ In NO ν A and T2K the matter effects induced by sterile neutrino oscillations are very small. Notwithstanding, for the sake of precision, they are fully incorporated in our simulations. A detailed description of the matter effects can be found in [33].

III. DATA USED AND DETAILS OF THE STATISTICAL ANALYSIS

We have considered the latest datasets of T2K and NO ν A from [61, 62] and [63], respectively. The disappearance channel of T2K is composed of 243 ν_μ - and 140 $\bar{\nu}_\mu$ -like events. The former (latter) are split into 28 (19) equally spaced energy bins in the range [0.2, 3.0] ([0.15, 3.0]) GeV. The appearance channel consists of three event samples: 75 ν_e -like events without pions, 15 $\bar{\nu}_e$ -like events without pions and 15 ν_e -like events with one pion in the final state. The first two samples are split into 23 equally spaced energy bins in the range [0.1, 1.25] GeV, whereas the last one consists of 16 bins in the range [0.45, 1.25] GeV. For both channels we extract the distribution of each background components from slide 17 in [61].

The dataset for the disappearance channel of NO ν A is presented into four quartiles for both the neutrinos and antineutrinos. Each quartile is split into 19 unequally spaced energy bins in the range [0.75, 4.0] GeV as shown in [63]. In total NO ν A has recorded 113 ν_μ - and 102 $\bar{\nu}_\mu$ -like events. We extract the background spectra from [63]. The dataset for the appearance channel is composed of three samples. Two of them are selected by the particle identification variable (low-PID and high-PID) introduced in the context of the convolutional neural network technique for event classification [64, 65]. The third one is the so-called “peripheral” sample. Each of the first two samples is further distributed into six equally spaced energy bins in the range [1.0, 4.0] GeV. In total NO ν A collected 58 ν_e - and 27 $\bar{\nu}_e$ -like events. We extract the background spectra from [63].

The analysis presented in this work is performed using the GLoBES software [66, 67], together with its new-physics package [68]. The sterile neutrino effects are included both in the $\nu_\mu \rightarrow \nu_e$ appearance channel, and in the $\nu_\mu \rightarrow \nu_\mu$ disappearance one. This holds both for neutrino and antineutrino modes. We have fixed the solar oscillation parameters θ_{12} and Δm_{21}^2 at their best fit values taken from the recent global fit [69]. The constraint on the reactor mixing angle θ_{13} is incorporated as an external gaussian prior likelihood estimated from [69]. The atmospheric oscillations parameters θ_{23} and Δm_{31}^2 and the CP-phase δ_{13} are treated as free parameters and are marginalized away when needed. Concerning the mixing angles that involve the fourth state, we have fixed them to the values $\theta_{14} = \theta_{24} = 8^\circ$ and $\theta_{34} = 0$. These are very close to the best estimates obtained in the global SBL analyses performed within the 3+1 scheme [7–10]. Concerning the CP phase δ_{14} , we vary its value in the range $[0, 2\pi]$. The CP-phase δ_{34} has been taken equal to zero, but in any case the analysis is not sensitive to it by construction, since we have set the associated mixing angle $\theta_{34} = 0$.² We set the mass-squared splitting to $\Delta m_{41}^2 = 1 \text{ eV}^2$, which is close to the value currently indicated by the SBL data. However, we underline that our findings would be unaltered for different values of such a parameter, provided that $\Delta m_{41}^2 > 0.1 \text{ eV}^2$. For such values, the fast oscillations induced by the large mass-squared splitting get totally averaged by the finite energy resolution of the detector. For the same motivation, the LBL setups are insensitive to the sign of Δm_{41}^2 and this allows us to confine our study to positive values. We have set the line-averaged constant Earth matter density³ of 2.8 g/cm^3 for all the LBL experiments considered. In our simulations, we have incorporated a full spectral analysis by making use of the binned events spectra for each LBL experiment. In the statistical analysis, the Poissonian $\Delta\chi^2$ has been marginalized over the systematic uncertainties using the pull method as prescribed in Refs. [71, 72].

IV. NUMERICAL RESULTS

First of all, we comment on how much the quality of the fit improves in the 4-flavor case with respect to the 3-flavor scheme. We find an improvement of $\Delta\chi^2 \sim 1.9$ in NO and $\Delta\chi^2 \sim 3.1$ in IO. This means that the hypothesis of a light sterile neutrino is preferred at the 1.4σ level in NO and 1.8σ level in IO. Although interesting, these numbers are low if compared with the indications arising from the SBL experiments, which have recorded anomalies having statistical significance in the $[2\sigma, 4\sigma]$ ballpark. However, we can expect some gain in sensitivity to arise from future data of NO ν A and T2K, and of course from the next-generation LBL facilities DUNE, T2HK and ESS ν SB.

The upper (lower) panels of Fig. 1 report the estimates of the oscillation parameters attained by expanding the χ^2 around the minimum value obtained when the 3-flavor (4-flavor) hypothesis is accepted as true. The projections refer to δ_{13} (left panels), θ_{23} (middle panels), and $|\Delta m_{31}^2|$ (right panels), and are derived by combining T2K and NO ν A data with an external prior on θ_{13} as derived from reactors. The upper (lower) panels refer to the 3-flavor (4-flavor)

² We recall that in vacuum the $\nu_\mu \rightarrow \nu_e$ transition probability is independent of θ_{34} (and δ_{34}). In matter, one expects a tiny dependence, which is very small in NO ν A and in T2K (see the appendix of [33] for a detailed discussion). As shown in [39], at DUNE, where matter effects are more pronounced, it will be possible to probe the CP-phase δ_{34} provided that θ_{34} is very large and close to its upper limit ($\sim 21^\circ$ at the 90% C.L. [9]).

³ The line-averaged constant Earth matter density has been computed using the Preliminary Reference Earth Model (PREM) [70].

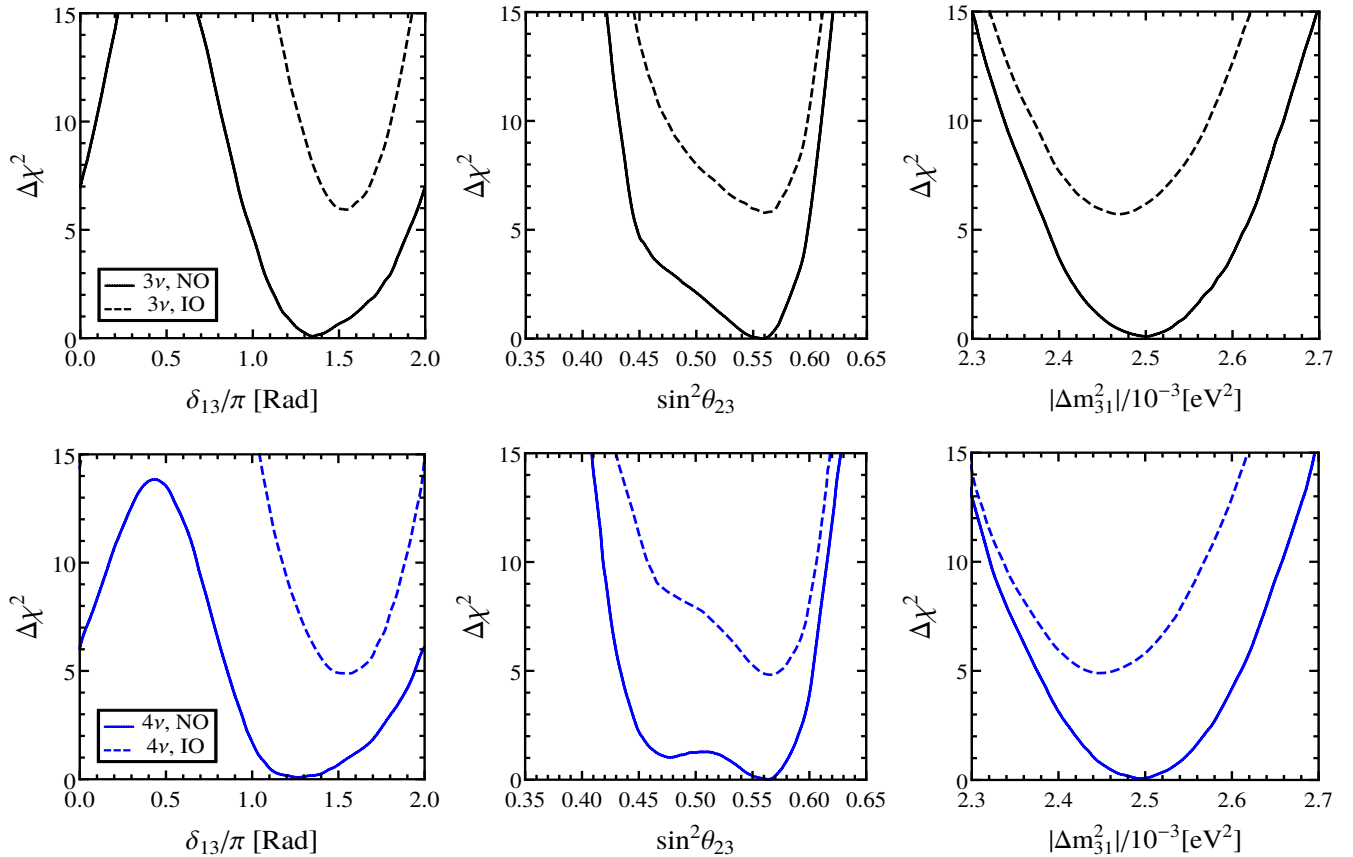


FIG. 1: Estimates of the oscillation parameters for the 3-flavor (upper panels) and 4-flavor (lower panels) scenarios determined by the combination of T2K and NO ν A (with reactor constraint). The continuous (dashed) curves refer to NO (IO).

case. In all panels, the continuous (dashed) curve represents the NO (IO). This figure shows that the 3-flavor ($\sim 2.4\sigma$) indication in favor of the normal ordering remains almost unchanged in the 3+1 scheme ($\sim 2.2\sigma$). The inspection of the left panels shows that in the normal ordering, the indication in favor of CP-violation (i.e. $\delta \neq 0, \pi$) found in the 3-flavor framework ($\sim 2.0\sigma$ with best fit $\delta_{13} \sim 1.35\pi$) decreases in the 3+1 scheme ($\sim 1.2\sigma$ with best fit $\delta_{13} \sim 1.28\pi$). Concerning the atmospheric mixing angle θ_{23} (middle panels) we see that, regardless of the NMO, the best fit lies in the higher octant ($\sin^2\theta_{23} \sim 0.56$) in both 3-flavor and 4-flavor scenarios. In the 4-flavor scheme there is a local minimum in the lower octant for $\sin^2\theta_{23} \sim 0.48$.⁴ This value is disfavored only at the $\sim 1.0\sigma$ ($\sim 1.6\sigma$) level in NO (IO) if compared to the best fit in the higher octant. On the other hand, in the 3-flavor scheme, the value $\sin^2\theta_{23} \sim 0.48$ is disfavored at the $\sim 1.7\sigma$ ($\sim 1.9\sigma$) level in NO (IO). Therefore, the preference for the higher octant of θ_{23} sensibly decreases in the presence of a sterile neutrino, especially in the NO. This is in agreement with the behavior predicted in the forecast study [40]. Finally, in the right panels we report the estimate of the atmospheric mass-squared Δm_{31}^2 splitting. From these plots we can observe that in NO the best fit value is very similar in 3-flavor and 4-flavor schemes, with a slight difference for the low values of the parameter. In IO both best fit and allowed range in the 4-flavor case are slightly shifted towards lower values with respect to the 3-flavor scenario.

In order to better understand how the 1-dimensional constraints shown in Fig. 1 arise, it is useful to look at the 2-dimensional projections in the plane spanned by a couple of oscillation parameters. In addition, such plots will enrich our comprehension by evidencing potential correlations among the oscillation parameters. Figure 2 displays the constraints in the plane spanned by θ_{13} and δ_{13} . Left (right) panel refers to NO (IO). The black contours represent the 3-flavor case, while the filled regions refer to the 4-flavor scenario. In both cases we show the 68% and 90% C.L. for two d.o.f.. Differently from all other plots, in this figure, we have drawn the regions allowed by NO ν A and T2K *without* the external prior on θ_{13} coming from reactor experiments. Such a prior is shown at the 1σ level as a thin

⁴ Note that for IO $\sin^2\theta_{23} \sim 0.48$ is an inflection point.

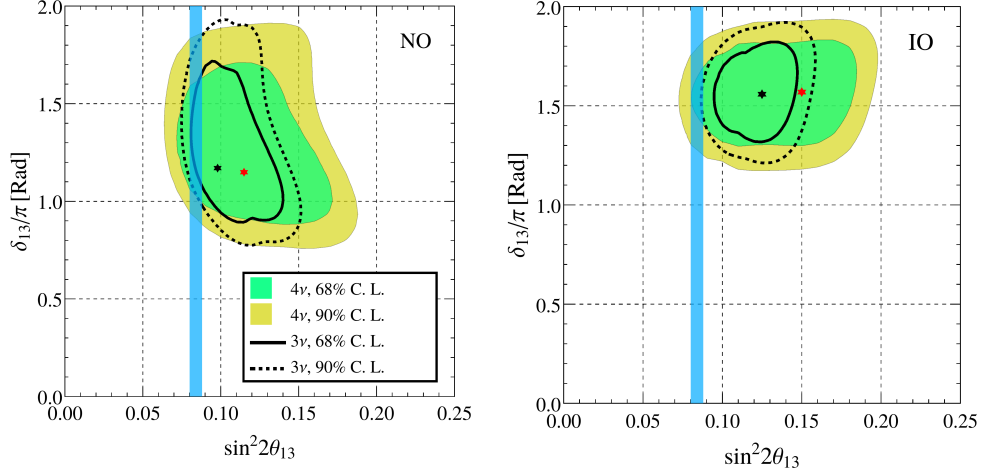


FIG. 2: Allowed regions obtained from the combination of T2K and NO ν A (without reactor constraint) in the plane spanned by $\sin^2 2\theta_{13}$ and δ_{13} . Left (right) panel refers to NO (IO). The black contours represent the 3-flavor case, while the filled regions pertain to the 4-flavor scheme. The vertical band indicates the 1σ constraint on θ_{13} from reactor experiments.

vertical band in each of the two panels of Fig. 2. This figure allows us to appreciate the synergy between reactor and accelerator constraints. In particular, one can observe how the level of superposition of the reactor band with the allowed regions of the LBL experiment, is bigger in the NO with respect to the IO. Therefore, the combination of reactor and LBL experiments tends to favor NO over IO. In the 4-flavor case the level of superposition is slightly enhanced both in NO and IO, but one still expects a preference for NO. Concerning the CP-phase δ_{13} , we see that the two LBL experiments tend to favor values of δ_{13} close to $\sim 1.2\pi$ for NO and $\sim 1.5\pi$ in IO. The combination with reactor data basically reinforces such preferences. More precisely in NO, where there is a slight negative correlation among θ_{13} and δ_{13} , one expects a best fit of δ_{13} close to $\sim 1.3\pi$. In IO there is almost no correlation among θ_{13} and δ_{13} , and one expects that best fit of δ_{13} will be unaltered $\sim 1.5\pi$. These findings help to explain the 1-dimensional projections in the left panels of Fig 1.

Figure 3 shows the constraints in the plane spanned by θ_{23} and $|\Delta m_{31}^2|$. Left (right) panel refers to NO (IO). The black contours represent the 3-flavor case, while the filled regions refer to the 4-flavor scenario. In both cases we show the 68% and 90% C.L. for two d.o.f.. As expected, the allowed regions are larger in 4-flavor than in 3-flavor scheme. This is natural as one has more freedom in the fit in the 3+1 scheme. However, one can notice that the range allowed

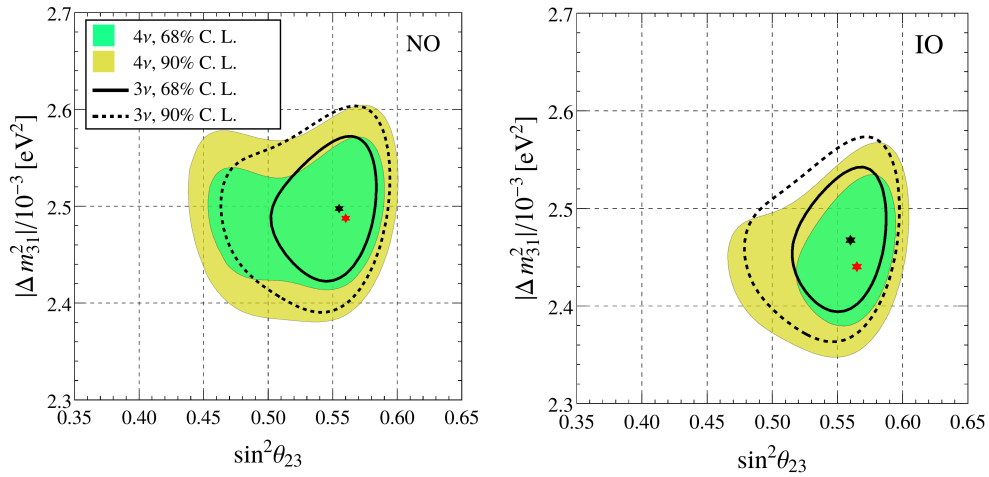


FIG. 3: Allowed regions obtained from the combination of T2K and NO ν A (with reactor constraint) in the plane spanned by $\sin^2 \theta_{23}$ and $|\Delta m_{31}^2|$. Left (right) panel refers to NO (IO). The black contours represent the 3-flavor case, while the filled regions pertain to the 4-flavor scheme.

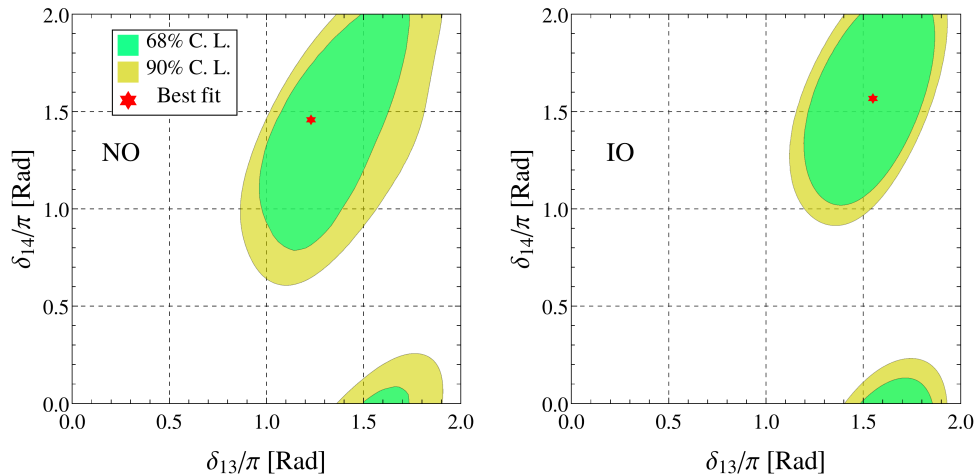


FIG. 4: Regions allowed by the combination of T2K and NO ν A (with reactor constraint) the plane spanned by the two CP-phases δ_{13} and δ_{14} . Left (right) panel refers to NO (IO).

for $|\Delta m_{31}^2|$ is very similar in the two scenarios, with a slight shift towards lower values in 4-flavor, which is more marked in the IO. This feature can be understood recalling that the Δm_{31}^2 is constrained mostly by the disappearance channel, which probes the $\nu_\mu \rightarrow \nu_\mu$ survival probability that is almost insensitive to the presence of sterile neutrinos. Concerning the atmospheric mixing angle θ_{23} , in the NO case, the rejection of the lower octant is less pronounced in the 4-flavor case with respect to the 3-flavor scenario.

Figure 4 displays the constraints in the plane spanned by the two CP-phases δ_{13} and δ_{14} for NO (left panel) and IO (right panel). In both mass orderings the CP-conserving cases $\delta_{14} = (0, \pi)$ are allowed at the 90% confidence level. We note that the two CP-phases have nearly the same best fit value in both mass orderings $\delta_{13} \sim \delta_{14} \sim 3\pi/2$. This behavior can be understood by observing that T2K presents a remarkable excess of electron neutrino events and, as already noticed in the analysis performed in [73], it has a dominant role in the fit. Inspecting the oscillation probability, one finds that both interference terms P_I^{INT} [in Eq. (6)] and P_{II}^{INT} [in Eq. (7)] assume the maximum positive value for $\delta_{13} = \delta_{14} = 3\pi/2$ both in NO and IO. Therefore, such values of the CP-phases guarantee a better agreement of the model with the data. This is also at the root of the positive correlation between the two CP-phases evidenced in both panels of Fig. 4. Time will tell us if this tendency is corroborated or not by future data.

V. CONCLUSIONS

We have considered the impact of a light sterile neutrino in the interpretation of the latest data of the long baseline experiments NO ν A and T2K. We have assessed the estimates of the standard 3-flavor parameters, highlighting the perturbations induced in 4-flavor scheme. We have shown that the indication of nearly maximal CP-violation found in the 3-flavor framework ($\delta_{13} \sim 3\pi/2$) holds with a smaller statistical significance in the 3+1 scheme. Concerning the neutrino mass ordering, the 3-flavor indication in favor of the normal ordering is almost unaffected in the 4-flavor scheme. The preference for the higher octant of θ_{23} sensibly decreases in the presence of a sterile neutrino. We have also pointed out that it is possible to constrain the new CP-phase δ_{14} , which intriguingly has best fit similar to the CP phase δ_{13} . Finally, we have evidenced the existence of a positive correlation among the standard CP-phase δ_{13} and the new CP-phase δ_{14} . We hope that our work may trigger more complete 4-flavor analyses incorporating also the atmospheric neutrino data, which are expected to be sensitive both to the NMO and to the standard and non-standard CP-phases δ_{13} and δ_{14} . However, we point out, that an accurate 4-flavor analysis of the current atmospheric data can be performed only from inside the experimental collaborations. To this regard, we would like to underline that the publication by the experimental collaborations of a χ^2 map for the 4-flavor analysis (as already available for the 3-flavor case), would be extremely useful, since it would allow one to perform a global analysis of all data sensitive to the NMO and (ordinary and new) CP-phases. In the eventuality of a discovery of a light sterile neutrino at SBL experiments, the availability of such pieces of information would become an indispensable tool for exploring the 4-flavor framework.

Acknowledgments

A.P. acknowledges partial support by the research grant number 2017W4HA7S “NAT-NET: Neutrino and Astroparticle Theory Network” under the program PRIN 2017 funded by the Italian Ministero dell’Istruzione, dell’Università e della Ricerca (MIUR) and by the research project *TAsP* funded by the Istituto Nazionale di Fisica Nucleare (INFN).

-
- [1] K. N. Abazajian et al. (2012), 1204.5379.
 - [2] A. Palazzo, Mod. Phys. Lett. **A28**, 1330004 (2013), 1302.1102.
 - [3] S. Gariazzo, C. Giunti, M. Laveder, Y. F. Li, and E. M. Zavanin, J. Phys. **G43**, 033001 (2016), 1507.08204.
 - [4] C. Giunti, Nucl. Phys. **B908**, 336 (2016), 1512.04758.
 - [5] C. Giunti and T. Lasserre, Ann. Rev. Nucl. Part. Sci. **69**, 163 (2019), 1901.08330.
 - [6] S. Bser, C. Buck, C. Giunti, J. Lesgourgues, L. Ludhova, S. Mertens, A. Schukraft, and M. Wurm, Prog. Part. Nucl. Phys. **111**, 103736 (2020), 1906.01739.
 - [7] F. Capozzi, C. Giunti, M. Laveder, and A. Palazzo, Phys. Rev. **D95**, 033006 (2017), 1612.07764.
 - [8] S. Gariazzo, C. Giunti, M. Laveder, and Y. F. Li, JHEP **06**, 135 (2017), 1703.00860.
 - [9] M. Dentler, A. Hernandez-Cabezudo, J. Kopp, P. A. N. Machado, M. Maltoni, I. Martinez-Soler, and T. Schwetz, JHEP **08**, 010 (2018), 1803.10661.
 - [10] A. Diaz, C. A. Argüelles, G. H. Collin, J. M. Conrad, and M. H. Shaevitz (2019), 1906.00045.
 - [11] A. Aguilar-Arevalo et al. (LSND), Phys. Rev. **D64**, 112007 (2001), hep-ex/0104049.
 - [12] A. A. Aguilar-Arevalo et al. (MiniBooNE), Phys. Rev. Lett. **121**, 221801 (2018), 1805.12028.
 - [13] G. Mention, M. Fechner, T. Lasserre, T. Mueller, D. Lhuillier, et al., Phys. Rev. **D83**, 073006 (2011), 1101.2755.
 - [14] W. Hampel et al. (GALLEX), Phys. Lett. **B420**, 114 (1998).
 - [15] J. N. Abdurashitov et al., Phys. Rev. **C73**, 045805 (2006), nucl-ex/0512041.
 - [16] Y. J. Ko et al. (NEOS), Phys. Rev. Lett. **118**, 121802 (2017), 1610.05134.
 - [17] M. Danilov (DANSS), in *2019 European Physical Society Conference on High Energy Physics (EPS-HEP2019) Ghent, Belgium, July 10-17, 2019* (2019), 1911.10140.
 - [18] A. P. Serebrov et al. (NEUTRINO-4), Pisma Zh. Eksp. Teor. Fiz. **109**, 209 (2019), [JETP Lett.109,no.4,213(2019)], 1809.10561.
 - [19] A. Palazzo, Phys. Rev. **D83**, 113013 (2011), 1105.1705.
 - [20] A. Palazzo, Phys. Rev. **D85**, 077301 (2012), 1201.4280.
 - [21] C. Giunti and Y. F. Li, Phys. Rev. **D80**, 113007 (2009), 0910.5856.
 - [22] P. Adamson et al. (MINOS), Phys. Rev. Lett. **117**, 151803 (2016), 1607.01176.
 - [23] P. Adamson et al. (MINOS+), Phys. Rev. Lett. **122**, 091803 (2019), 1710.06488.
 - [24] P. Adamson et al. (NOvA), Phys. Rev. **D96**, 072006 (2017), 1706.04592.
 - [25] K. Abe et al. (T2K), Phys. Rev. **D99**, 071103 (2019), 1902.06529.
 - [26] F. P. An et al. (Daya Bay), Phys. Rev. Lett. **117**, 151802 (2016), 1607.01174.
 - [27] J. Ashenfelter et al. (PROSPECT), Phys. Rev. Lett. **121**, 251802 (2018), 1806.02784.
 - [28] H. Almazn Molina et al. (STEREO) (2019), 1912.06582.
 - [29] K. Abe et al. (Super-Kamiokande), Phys. Rev. **D91**, 052019 (2015), 1410.2008.
 - [30] M. G. Aartsen et al. (IceCube), Phys. Rev. Lett. **117**, 071801 (2016), 1605.01990.
 - [31] M. G. Aartsen et al. (IceCube), Phys. Rev. **D95**, 112002 (2017), 1702.05160.
 - [32] A. Albert et al. (ANTARES), JHEP **06**, 113 (2019), 1812.08650.
 - [33] N. Klop and A. Palazzo, Phys. Rev. **D91**, 073017 (2015), 1412.7524.
 - [34] A. Palazzo, Phys. Lett. B **757**, 142 (2016), 1509.03148.
 - [35] S. K. Agarwalla, S. S. Chatterjee, A. Dasgupta, and A. Palazzo, JHEP **02**, 111 (2016), 1601.05995.
 - [36] D. Hollander and I. Mocioiu, Phys. Rev. **D91**, 013002 (2015), 1408.1749.
 - [37] J. M. Berryman, A. de Gouvêa, K. J. Kelly, and A. Kobach, Phys. Rev. **D92**, 073012 (2015), 1507.03986.
 - [38] R. Gandhi, B. Kayser, M. Masud, and S. Prakash, JHEP **11**, 039 (2015), 1508.06275.
 - [39] S. K. Agarwalla, S. S. Chatterjee, and A. Palazzo, JHEP **09**, 016 (2016), 1603.03759.
 - [40] S. K. Agarwalla, S. S. Chatterjee, and A. Palazzo, Phys. Rev. Lett. **118**, 031804 (2017), 1605.04299.
 - [41] P. Coloma, D. V. Forero, and S. J. Parke, JHEP **07**, 079 (2018), 1707.05348.
 - [42] S. Choubey, D. Dutta, and D. Pramanik, Phys. Rev. D **96**, 056026 (2017), 1704.07269.
 - [43] S. Choubey, D. Dutta, and D. Pramanik, Eur. Phys. J. C **78**, 339 (2018), 1711.07464.
 - [44] S. K. Agarwalla, S. S. Chatterjee, and A. Palazzo, JHEP **04**, 091 (2018), 1801.04855.
 - [45] N. Haba, Y. Mimura, and T. Yamada, Phys. Rev. D **101**, 075034 (2020), 1812.10940.
 - [46] S. Kumar Agarwalla, S. S. Chatterjee, and A. Palazzo, JHEP **12**, 174 (2019), 1909.13746.
 - [47] A. Palazzo, Universe **6**, 41 (2020).
 - [48] A. Donini and D. Meloni, Eur. Phys. J. **C22**, 179 (2001), hep-ph/0105089.
 - [49] A. Donini, M. Lusignoli, and D. Meloni, Nucl. Phys. **B624**, 405 (2002), hep-ph/0107231.
 - [50] A. Donini, M. Maltoni, D. Meloni, P. Migliozi, and F. Terranova, JHEP **12**, 013 (2007), 0704.0388.

- [51] A. Dighe and S. Ray, Phys. Rev. **D76**, 113001 (2007), 0709.0383.
- [52] A. Donini, K.-i. Fuki, J. Lopez-Pavon, D. Meloni, and O. Yasuda, JHEP **08**, 041 (2009), 0812.3703.
- [53] O. Yasuda, in *Physics beyond the standard models of particles, cosmology and astrophysics. Proceedings, 5th International Conference, Beyond 2010, Cape Town, South Africa, February 1-6, 2010* (2011), pp. 300–313, 1004.2388, URL <http://inspirehep.net/record/851933/files/arXiv:1004.2388.pdf>.
- [54] D. Meloni, J. Tang, and W. Winter, Phys. Rev. **D82**, 093008 (2010), 1007.2419.
- [55] B. Bhattacharya, A. M. Thalapillil, and C. E. M. Wagner, Phys. Rev. **D85**, 073004 (2012), 1111.4225.
- [56] A. Donini, P. Hernandez, J. Lopez-Pavon, M. Maltoni, and T. Schwetz, JHEP **07**, 161 (2012), 1205.5230.
- [57] R. Gandhi, B. Kayser, S. Prakash, and S. Roy, JHEP **11**, 202 (2017), 1708.01816.
- [58] P. F. de Salas, D. V. Forero, C. A. Ternes, M. Tortola, and J. W. F. Valle, Phys. Lett. **B782**, 633 (2018), 1708.01186.
- [59] F. Capozzi, E. Lisi, A. Marrone, and A. Palazzo, Prog. Part. Nucl. Phys. **102**, 48 (2018), 1804.09678.
- [60] I. Esteban, M. C. Gonzalez-Garcia, A. Hernandez-Cabezudo, M. Maltoni, and T. Schwetz, JHEP **01**, 106 (2019), 1811.05487.
- [61] G. Žárnecki, Talk at Les Rencontres de Physique de la Vallée d’Aoste, 10-16 March 2019, La Thuile, Italy (2019), URL <https://www.t2k.org/docs/talk/337/cpv-lathuile2019>.
- [62] K. Abe et al. (T2K), Nature **580**, 339 (2020), 1910.03887.
- [63] M. Acero et al. (NOvA), Phys. Rev. Lett. **123**, 151803 (2019), 1906.04907.
- [64] A. Aurisano, A. Radovic, D. Rocco, A. Himmel, M. D. Messier, E. Niner, G. Pawloski, F. Psihas, A. Sousa, and P. Vahle, JINST **11**, P09001 (2016), 1604.01444.
- [65] F. Psihas, E. Niner, M. Groh, R. Murphy, A. Aurisano, A. Himmel, K. Lang, M. D. Messier, A. Radovic, and A. Sousa (2019), 1906.00713.
- [66] P. Huber, M. Lindner, and W. Winter, Comput.Phys.Commun. **167**, 195 (2005), hep-ph/0407333.
- [67] P. Huber, J. Kopp, M. Lindner, M. Rolinec, and W. Winter, Comput.Phys.Commun. **177**, 432 (2007), hep-ph/0701187.
- [68] J. Kopp, <https://www.mpi-hd.mpg.de/personalhomes/globes/tools/snu-1.0.pdf> (2010).
- [69] F. Capozzi, E. Di Valentino, E. Lisi, A. Marrone, A. Melchiorri, and A. Palazzo (2020), 2003.08511.
- [70] A. M. Dziewonski and D. L. Anderson, Physics of the Earth and Planetary Interiors **25**, 297 (1981).
- [71] P. Huber, M. Lindner, and W. Winter, Nucl. Phys. **B645**, 3 (2002), hep-ph/0204352.
- [72] G. L. Fogli, E. Lisi, A. Marrone, D. Montanino, and A. Palazzo, Phys. Rev. **D66**, 053010 (2002), hep-ph/0206162.
- [73] F. Capozzi, S. S. Chatterjee, and A. Palazzo, Phys. Rev. Lett. **124**, 111801 (2020), 1908.06992.